Available online on 15.02.2023 at http://jddtonline.info

Journal of Drug Delivery and Therapeutics

Open Access to Pharmaceutical and Medical Research

Open Access Full Text Article

Research Article

Characterization, antibacterial and anticancer study of silk fibroin hydrogel

Vandana Singh [1, 2], Devika Srivastava[1], Prashant Pandey[3], Mukesh Kumar[1], Sachin Yadav[4], Dinesh Kumar[2], Venkatesh Kumar R.[1]*

1. *Department of Zoology, Babasaheb Bhimaro Ambedkar University, Raibereli road, Lucknow, U.P, India-226025*
2. *Centre for Biomedical Research, SGPGIMS Campus Raibereli road, Lucknow, U.P, India-226014.*
3. *Department of Pharmaceutical sciences , Babasaheb Bhimaro Ambedkar University, Raibereli road, Lucknow, U.P, India-226025*
4. *Department of Chemistry, Integral University, Lucknow-226026*

Article Info:

Article History:

Received 06 Dec 2022
Reviewed 21 Jan 2023
Accepted 23 Jan 2023
Published 15 Feb 2023

Cite this article as:

Singh V, Srivastava D, Pandey P, Kumar M, Yadav S, Kumar D, Venkatesh Kumar R, Characterization, antibacterial and anticancer study of silk fibroin hydrogel, Journal of Drug Delivery and Therapeutics. 2023; 13(2):21-31

DOI: http://dx.doi.org/10.22270/jddt.v13i2.5733

*Address for Correspondence:

Dr. Venkatesh Kumar R., Associate Professor Babasaheb Bhimrao Ambedkar University (A Central University), VidyaVihar, Raebareli Road, Lucknow, U.P. 226025, India

Abstract

Purpose: Protein-based hydrogels such as silk fibroin hydrogel, are used in tissue engineering and regenerative medicine applications as they showed striking characteristics like biocompatibility and offered various benefits as biomaterials. The current study sought to prepare silk fibroin hydrogel and characterise it in order to assess its antibacterial and anticancer activity.

Methodology: Silk fibroin hydrogel was prepared and characterized by using different microscopy methods, namely Scanning Electron Microscopy (SEM), Phase Contrast Electron (PCM) microscopy, and foldscope analysis. Further, it was characterized through 1H-NMR analysis, Fourier Transform Infrared spectroscopy (FTIR) analysis, and swelling properties. A Current study also covers an antimicrobial and anticancer analysis of silk fibroin hydrogel by disk diffusion method and SRB (Sulforhodamine B) assay respectively.

Results: The antibacterial study confirmed that SF hydrogel has a moderate antibacterial activity for *Streptococcus mutans,* and *Salmonella typhi.* Additionally, the SRB assay test showed that silk fibroin hydrogels had moderate anticancer activity against the human lung cancer cell line (A549).

Conclusion: The current study unequivocally demonstrates that silk fibroin hydrogel has antibacterial and anti-cancerous properties, making it a suitable scaffold for future studies that seek to target a specific drug delivery site.

Keywords: Silk fibroin; Swelling behaviour; Anticancer; Drug carrier; Wound healing

Graphical Abstract

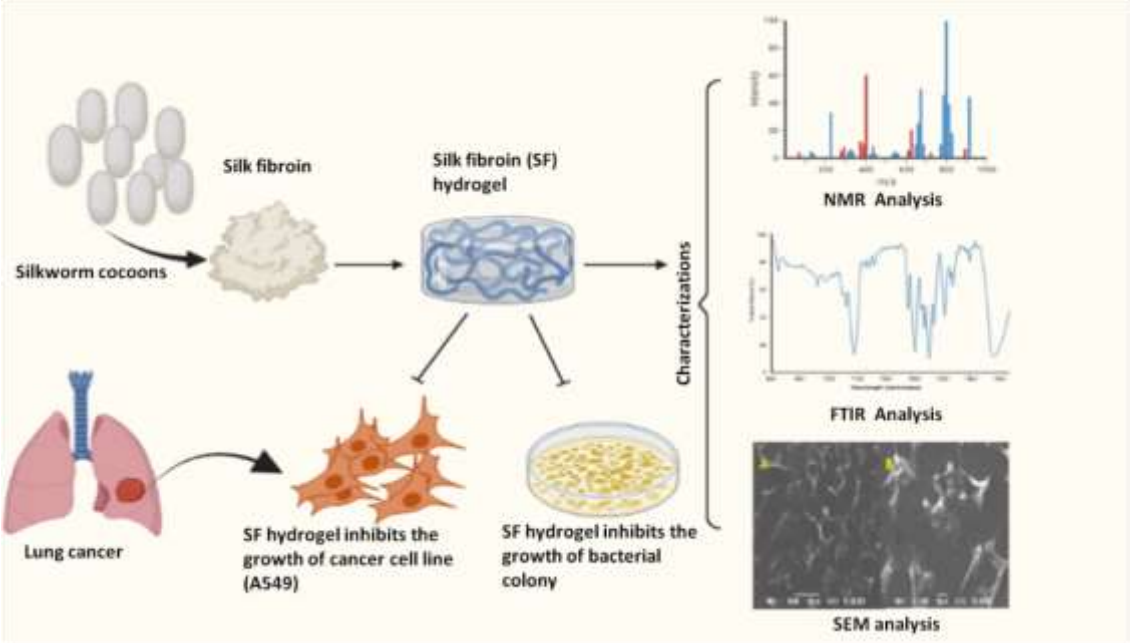

INTRODUCTION

Hydrogels are polymer networks that are cross-linked and have a high absorptive capacity (the moisture content can reach up to 70%) and resilience properties for swelling in non-dissolving aqueous solutions, making them suitable for cell and cytokine administration, large surface area for cell proliferation, cell adhesion, cell migration, and cell growth[1-4]. Hydrogels are usually applied in regenerative medicine, cartilage, nerve and bone regeneration, tissue engineering, and growth factor delivery[5-9]. Silk fibroin hydrogel is ubiquitous in hydrogel-related studies, due to which its importance cannot be ignored without citing its references in most of the studies.

Silk fibroin is made up of disulfide-linked heavy and light chains. The heavy chain is composed primarily of alanine and glycine, resulting in a water-insoluble chain (as shown in Fig. 1)[10]. Hydrophobic regions of short-side chain acids dominate the primary sequence. Typically, silk fibroin is made up of β-sheet structures, which are used for tightly packed protein slices with hydrogen-bonded antiparallel chains[11]. It is one of the most naturally occurring biodegradable materials having excellent water retention, freezing tolerance, exceptional pore size that plays an important role in nutrients and metabolites transport, interconnectivity among cells, permitting cellular growth and vascularization in the host, which would be greatly helpful in the biomedical field[12-17]. SF hydrogel also demonstrates high tensile strength, injectability, self-healing capacity, adherence property, permeability, responsiveness to environmental stimuli, 3D printability, etc[18- 21]. Biomaterial contamination by bacteria poses a severe threat to human health on a global scale. Therefore, SF hydrogels emerged as multifunctional biomaterials with antibacterial characteristics and the ability to resist infection[22]. Similarly, suppressing the growing tumor with the help of injectable SF hydrogel is gaining significant attention in cancer research and treatment by inhibiting the abrupt multiplication of most cancerous cells[23].

Therefore, in the current study, we have targeted some of the bacterial strains and cancerous cell lines to assess the antibacterial and anticancer properties of silk fibroin hydrogel based on the proven studies of earlier workers.

MATERIALS AND METHODS

Materials and reagents

The cocoons of the Indian silkworm *Bombyx mori* were obtained from the Central Sericulture Research and Training institute in Mysuru, Karnataka. Trimethyl-silyl-propionic acid sodium salt, Sigma-Aldrich deuterium oxide (D2O), deionized water, phosphate-buffered saline (PBS), antibiotics (VANCO), lithium bromide (LiBr) salt (Sigma-Aldrich).

Preparation of silk fibroin hydrogel

Two different protein types, fibroin, and sericin, are present in silkworm cocoons. To obtain silk fibroin (SF) protein, sericin must be removed three times with a 1 g/l Na2CO3 aqueous solution at 80˚ to 100˚ C for 30 to 45 minutes (as previously described by Rockwood et al, 2011). The fibroin strands were first dried in an oven at 65˚ to 80°C for 48 hours to obtain the silk fibroin (SF) solution, and then they were dissolved in a LiBr solution at a ratio of 1:4. (Silk fibroin: LiBr). After that, the dialyzing SF solution against deionized water for 48 to 72 hours to eliminate the LiBr salt, and its final concentration was 0.05 g/ml. The silk fibroin solution was prepared and stored at 4°C after filtering[14].

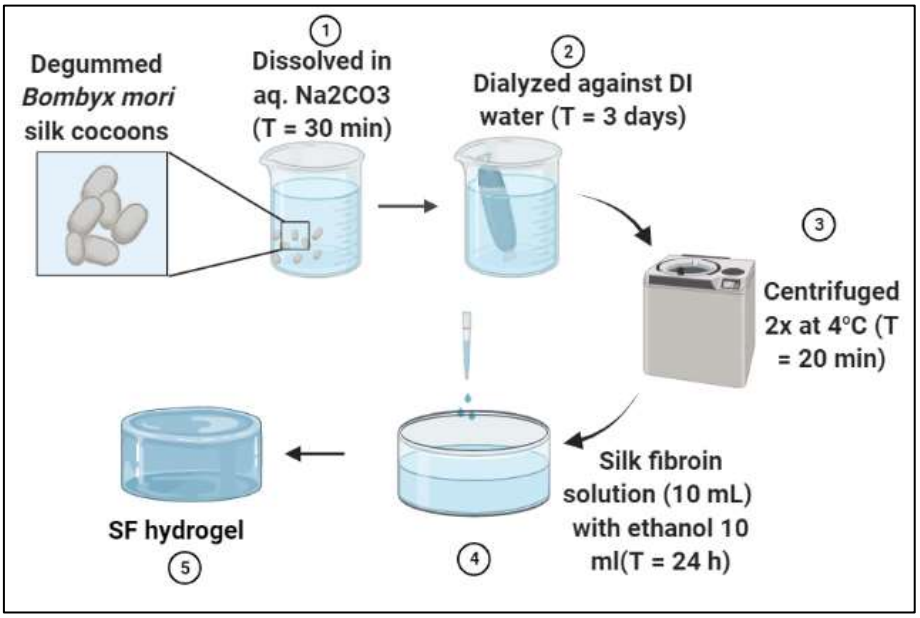

Figure 1: Silk fibroin hydrogel preparation from the silk cocoon of *Bombyx mori*

Samples characterization

Microscopic analysis

Scanning electron microscopy (JEOL, JSM 6490 LV Tokyo, Japan), phase contrast electron microscopy (Olympus CX21 Phase Contrast Microscope Polarized light equipped with Q-imaging micropublisher 3.3 RTV Camera, Japan), and foldscope microscopy were used to investigate the surface morphology of SF hydrogel. For SEM analysis, SF hydrogels were smeared on aluminium foil and fixed on aluminium stubs with double-sided carbon tape and the sample was examined under a scanning electron microscope at various magnifications. For phase contrast microscopy (PCM) analysis, SF hydrogel was smeared on glass slides and observed under a phase contrast microscope. The microphotographs were recorded at 20X resolution and digital images were saved for further analysis[24,25]. Furthermore, Foldscope is operated by mounting SF hydrogel on a microscope glass slide and then inserting the glass slide into the foldscope. The sample was observed by focusing through a focus ramp and viewing it with a mobile camera lens, after which the images were captured.

Swelling behaviour

Gravimetric analysis was used to determine the swelling properties of SF hydrogel. The sample was dried before being immersed in distilled water. Swollen SF hydrogel was removed from water and weighed at regular intervals. The SF hydrogel's swelling ratio (SR) was calculated using the formula:

SR = [(Wt-Wd)/ Wd],

where Wt = weight of swollen SF hydrogels at particular time t,

Wd = weight of dry samples.

pH calibration

Digital pH meter (Make: THERMO) was used to check the pH of SF hydrogel. Firstly, the electrodes of digital pH meter was dipped into the SF hydrogel and reading was recorded carefully under room temperature.

Infrared spectroscopy analysis

Fourier transform infrared (FT-IR) spectrometer (PerkinElmer Frontier) was to analyze the functional SF hydrogel. SF hydrogel was made in the form of pellets by using KBr then FTIR spectra recorded between 4000 and 400 cm^{-1}.

^{1}H NMR analysis

NMR spectra of raw silk SF protein solution was recorded at 300 K using 800 MHz NMR spectrometer (Bruker Biospin, Avance-III, Bruker Corporation, Silberstreifen 4, 76287 Rheinstetten, Germany). NMR spectrometer was operated at ^{1}H frequency of 800.21 MHz (equipped with 5 mm inverse detection TCI Cryoprobe and an actively shielded z-gradient with maximum output for gradient strength (53 G/cm). The 450 µL of silk SF protein solution was filled in 5mm NMR sealed tube and for locking and chemical shift reference, a sealed capillary tube containing 0.5 mM solution of trimethylsilyl propionate (TSP) prepared in 100% deuterium oxide (D_2O) was used. Bruker's standard pulse programme library sequences (zgesgp, cpmgpr1d and ledbpgp2s1d) were used to acquire 1D ^{1}H NMR spectra as per the parameters listed in **Table 1**.

Table 1: The various acquisition and processing parameters used for the NMR analysis of silk SF protein solution

Experiments	ZGESGP	CPMGPR1D (T2 filter time 66 ms)	LEDBPGP2S1D (diffusion time 60 ms)
Size of FID	32k	64k	32k
Number of Scans (NS)	64	64	128
Spectral width (ppm)	16.02	20.0267	12.02
Acquisition time (sec)	1.28 sec	2.05 sec	1.70 sec
Recycle delay (d1)	2 sec	4 sec	4 sec
Size of Real spectrum	64k	64k	64k
Experiment time	4 min 25 sec	8 min 11 sec	13 min 55 sec

Each free induction decay (FID) data point was zero-filled to a maximum of 64 K data points before the Fourier-transformation (FT). Further each FID was apodized with a sine–bell apodization function and a line broadening factor of 0.3 Hz before FT. The Bruker data processing software was used to process all NMR spectra. (Topspin v3.0), which included manual phase and baseline correction. After FT, the spectral peaks were calibrated to methyl peak of TSP at 0.0 ppm.

Antibacterial activity

The SF hydrogel was tested for organisms *(Bacillus cereus, Streptococcus mutans, Salmonella typhi and Pseudomonas aeruginosa*). In 4 Erlenmeyer flasks, 30mL of Luria Bertani (LB) broth (10g Tryptone, 10g NaCl, 6g yeast extract, 1000mL distilled water) was prepared by adding 0.3g tryptone, 0.3g sodium chloride, 0.18g yeast extract, 30mL distilled water and autoclaving at 121°C for 15 minutes. *Bacillus cereus* (MTCC 1272), *Streptococcus mutans* (MTCC 497), *Salmonella typhi* (MTCC 735), and *Pseudomonas aeruginosa* (MTCC 2453) were then inoculated in 30mL of sterilised LB broth and incubated for 24 hours at 37 C. Cultured organisms (*Bacillus cereus, Streptococcus mutans, Salmonella typhi, and Pseudomonas aeruginosa*) were centrifuged for 10 minutes at 6000rpm, supernatant was discarded, and pellets were dissolved in 1% (w/v) sodium chloride and adjusted to absorbance 1.000 at 600nm using a UV spectrophotometer (Genesys 10S UV-VIS Spectrophotometer). In 1mL of Dimethyl sulfoxide (DMSO), 10mg of SF hydrogel was dissolved. Pipetting 10L (100g), 20L (200g), 30L (300g), and 40L (400g) aliquots of the sample were taken, and the final volume was increased to 50L by adding DMSO. In an Erlenmeyer flask, 800mL of LB agar media (10g Tryptone, 10g NaCl, 6g yeast extract, 20g agar, 1000mL distilled water) was made by combining 8g of tryptone, 8g of sodium chloride, 4.8g of yeast extract, 16g of agar, 800mL of distilled water, and autoclaving at 121°C for 15 minutes. In the sterilised petriplates, 25mL of LB agar was poured and allowed to solidify. 200L of prepared inoculum (*Bacillus cereus, Streptococcus mutans, Salmonella typhi, and Pseudomonas aeruginosa)* was poured into each agar plate and thoroughly spread with a plate spreader. The borer was used to make 5 wells measuring 0.6 cm in each plate, and 50L of sample containing 100g, 200g, 300g, and 400g were placed in each well, along with 50L of DMSO was placed in the middle well as a control blank. The bacteria plates were kept in an incubator for 24 hours at 37°C. Later, the zone of inhibition was measured in millimetres (Millimeter)[26, 27].

Antifungal activity

The antifungal activity of all three extracts was evaluated against the pathogenic microbes, *A. flavus* and *A. brassicae*. The activity was evaluated by the method of disk diffusion. For this test, first of all for the fungus isolates the Potato Dextrose Agar (PDA) According to the standard composition (Himedia that is 40gms of the media was suspended in 1L water), the media was formed and autoclaved at 121ºC and 15psi for 15minutes using autoclave (Gentek India Pvt. Ltd.). Each plate was filled with 20ml of culture media after the sterilisation media was poured into sterile glass petri dishes using aseptic techniques

under Laminar air flow (Toshiba, India). The plates were allowed to solidify properly then the media was inoculated with the respective fungus isolate the fungal isolate *A. flavus* and *A. brassicae* on the PDA media by spread plate technique, for which 100µl culture broth of each isolate was poured into media and uniformly spread using sterile glass rod. The extract samples were prepared for concentration i.e., 100µg/ml, 200µg/ml, 300µg/ml in respective solvent or water. The disks were impregnated with this concentration of extracts and allowed to dry. Ten minutes after spreading, disk was place onto the media plates using sterile forceps. Allowing the samples to diffuse through the disk into the media and then the plates were sealed with parafilm and incubated at 27ºC from 48hrs to 5 days to obtain completely grown fungus. One of the positive controls on the plates had two wells that is Luliconazole antifungal agent of the concentration of 1200ppm and the negative control disk was loaded with water or solvent. Plates were observed for the clear zone around the disk called as the zone of inhibition, as well as the diameter of these zones was measured in mm and recorded.

Anticancer activity

SRB (Sulforhodamine B) assay was utilised to test anticancer activity of SF hydrogel against A549 cell lines [28]. A549 cell lines grown in medium **(**2% mM L-glutamine and 10% foetal bovine serum). In the present experiment, in 96 well microtiter plates, 5000 cells were added per well. After that, microtiter plates were kept in incubator (keeping the temperature at 37° C, the CO2 at 5%, the air at 95%, and the relative humidity at 100%) for 24 hours. SF hydrogel was also solubilized in appropriate solvent 100mg/ml diluted with water to 1mg/ml, and before use, kept frozen. A frozen aliquote was thawed and diluted to a concentration of 100, 200, 400, and 800 g/ml at the time of SF hydrogel addition. 10 µl aliquots of different SF hydrogel dilutions were inoculated to 90 µl medium containing microtiter to make final concentrations, such as 10, 20, 40, and 80 g/ml. cell lines were fixed by adding 30% (w/v) in 50 µl of cold to make TCA concentration of 10% and kept for 1hr at 4°C. Plates were cleaned with tap water five times after the removal of the supernatant, and then dried. 50µl of 0.4% (w/v) SRB solution in 1% acetic acid was inoculated into each well, then left at room temperature for 20 minutes. After the stain was finished, it was washed five times with 1% acetic acid, then air dried. 10 mM trizma base was used to elute the bound stain, then absorbance was measured at 540 nm with a reference wavelength of 690 nm, and then growth percentage was calculated. Growth percentage was calculated as the ratio of the test well's average absorbance to the control wells' average absorbance * 100. Using the six absorbance measurements, the growth percentage of each SF hydrogel concentration was calculated [the four concentration levels of SF hydrogel at time zero (Tz), control growth (C), and test growth (Ti)].Growth inhibition percent was determined as:

$$[Ti/C] \times 100\ \%$$

RESULTS AND DISCUSSION

Microscopic analysis

The surface morphology of SF hydrogel was examined by scanning electron microscopy (SEM), phase contrast microscopy (PCM), and foldscope. Our SEM, PCM, and foldscope results confirmed that SF hydrogel has an interconnected branching-like structure owing to the presence of β-sheet structure and forming a porous scaffold that aids in the transport of nutrients and oxygen, as shown in Figures 2.

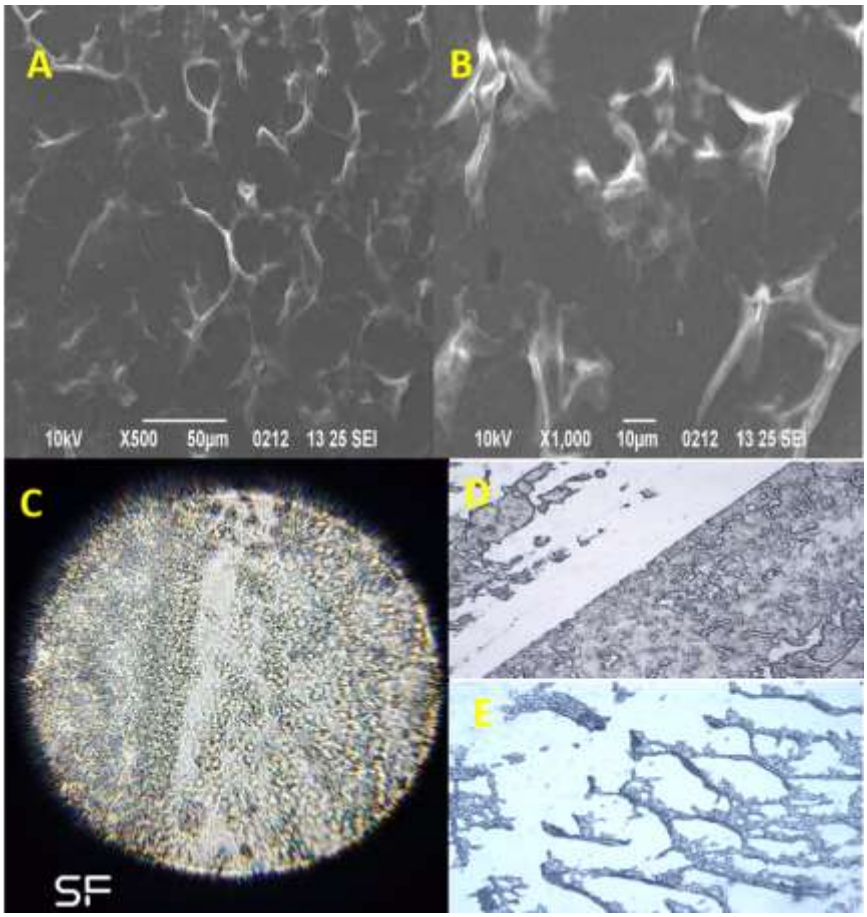

Figure 2: Morphological characteristics of SF hydrogel by using SEM analysis (A, B), foldscope (C) and PCM analysis (D, E)

pH calibration

The goal of this research is to look the pH responsive properties of SF hydrogel. The result showed that silk fibroin hydrogel pH was 6.24.

Swelling properties

One of the fundamental properties of SF hydrogels is their ability to swell. Curves of the swelling ratio with time of SF hydrogel were noted in table 2 and shown in Fig. 3 to investigate its swelling behaviour in distilled water at room temperature. Swelling rates of SF hydrogels were found to increase rapidly in the first 45 hours and then start decreasing to reach equilibrium. These multiple, large, and intertwined pores in SF hydrogels also contributed to a rapid rate of swelling and water retention. Although a higher SF concentration showed enhanced cross-linking in polymer and work against swelling ability [29].

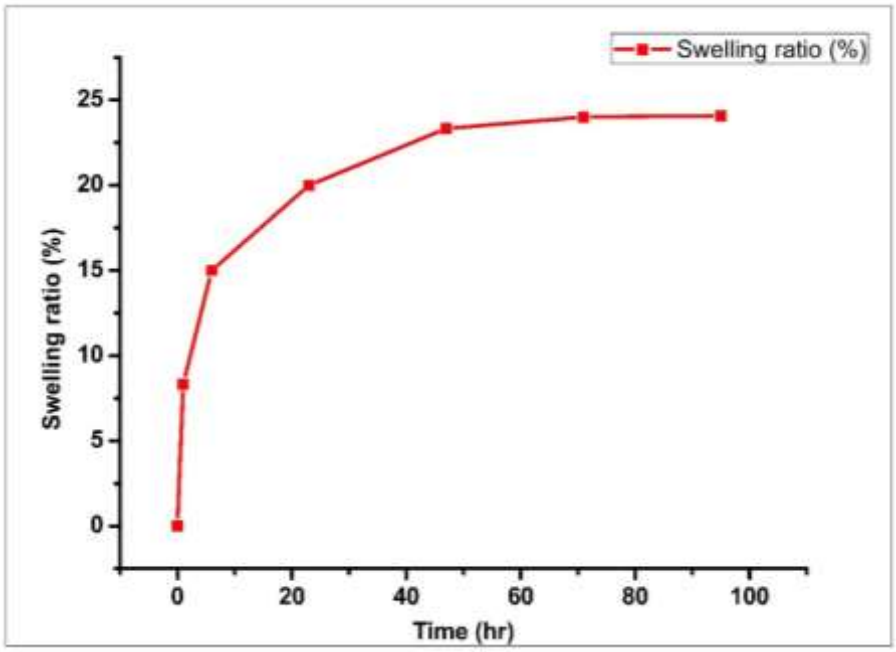

Figure 3: Swelling ratio percentage SF Hydrogels, having a rapid rate of swelling at 45 h and then become constant.

Table 2: Swelling weight of SF hydrogel with respect to time.

Sample	Swelling Weight	Time (hr)	Swelling ratio (%)
SF hydrogel	1.2	0	0
	1.3	1	8.33
	1.38	6	15
	1.44	23	20
	1.48	47	23.33
	1.488	71	24
	1.489	95	24.08

Infrared spectroscopy analysis

FTIR spectra was employed to investigate the functional group and chemical composition of SF hydrogel. The experimental outcomes are displayed in Figure 4. As evident from Fig. 4 three distinct bonds were identified in the SF hydrogel spectra at 1637, 1402, and 1326 cm-1, which were associated with amide I (CO vibration of stretching and NH bending in-plane), amide II (CN stretching vibration and NH in-plane bending), and amide III (CN stretching vibration and NH bending vibration) bonds. All of these typical absorbance peaks could be the result of a hydrogen-bonded NH group. The molecular structure of *B. mori* silk fibroin exhibits absorption peaks for the β-sheet at 1630, 1530, and 1240 cm-1, the random coil configuration at 1650 or 1645, 1550, and 1230 cm-1, and the α -helix at 1655 cm1. Peaks at 3300 cm-1 showed a change in intensity in response to hydrogen bonding. A β-sheet structure was suggested by absorption peak shifts of 1625–1630 cm-1 (amide I), 1520–1530 cm-1 (amide II), and 1265–1270 cm-1 (amide III). (Fig.4 and Table 3). The regenerated silk fibroins' FTIR spectrum revealed significant absorption peaks at 1230, 1620 and 1514, cm-1, which are the typical absorption peaks of β--sheets [30].

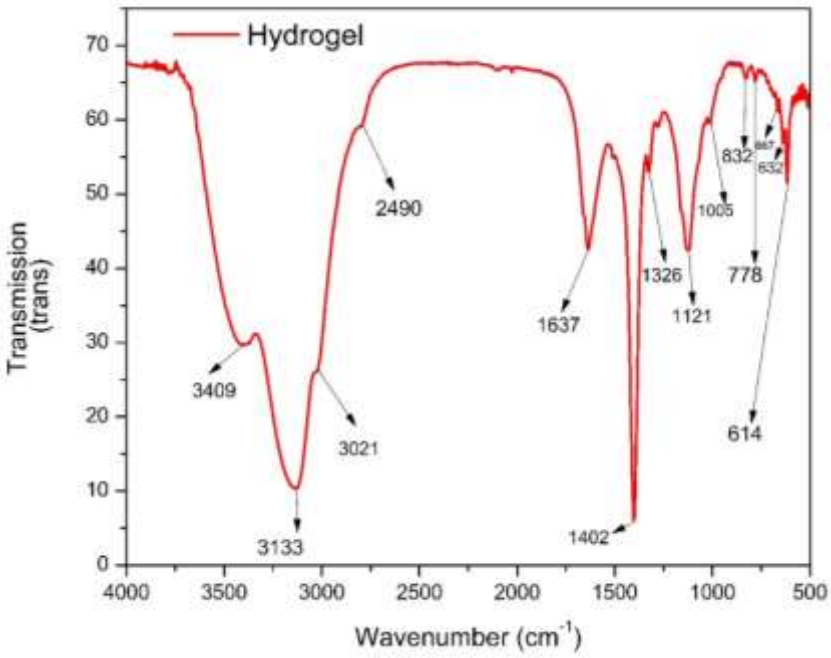

Figure 4: FTIR analysis of SF hydrogel

Table 3: FTIR wavenumber of SF hydrogel

Wavenumber	Types peak	Strength of peak	Compond
614	sharp	medium	CCl
632	sharp	weak	CCl
667	sharp	weak	CCl
778	sharp	weak	
832	Sharp	weak	=C-H
1005	broad	weak	Ether(C-O)
1121	sharp	medium	Ether (C-O),CN, glyosidic linkage
1326	sharp	weak	C-F
1402	sharp	high	C=C(aromatic)
1637	sharp	medium	C=C alkene, NH(Amide 1)
2490	broad	weak	
3021	broad	weak	=C-H aromatic C-H
3133	broad	high	Aromatic hydrocarbon ring, NH (amine and amide)
3409	broad	weak	OH group

1D ^{1}H NMR spectroscopy

NMR spectroscopy has proven to be highly useful in studying the structural and dynamic features of various globular and fibrous proteins, including silk fibroin hydrogel [31]. Here, we used three different 1D 1H NMR spectroscopy experiments to confirm the exquisite preparation of silk fibroin protein (Figure 5). Figure 5 shows an overlay of 1D and 1H NMR spectra recorded using Bruker standard RF pulse programs: (a) ZGESGP spectrum showing NMR signals from all the proton nuclei present in the solution sample, (b) CPMG showing NMR signals from all the proton nuclei exhibiting long T2 time (it may include low MW metabolites or highly flexible 1H spins of higher MW biological macromolecules such as proteins) and (c) diffusion edited 1D 1H NMR spectrum which filters out the NMR signals of molecules exhibiting very high diffusion and shows the NMR signal from slow diffusing (higher MW) biological macromolecules such as proteins. The NMR peaks annotated in different NMR spectra correspond to the flexible fragments of the SF polypeptide chain, including those corresponding to the N- or C-terminal arms. The NMR spectral signals were found in a close match with previous reports [32,33] and mainly represented the primary protein sequence of silk fibroin contains containing some amino acids (such as alanine, glycine, serine, tyrosine, and valine) are relatively more abundant.

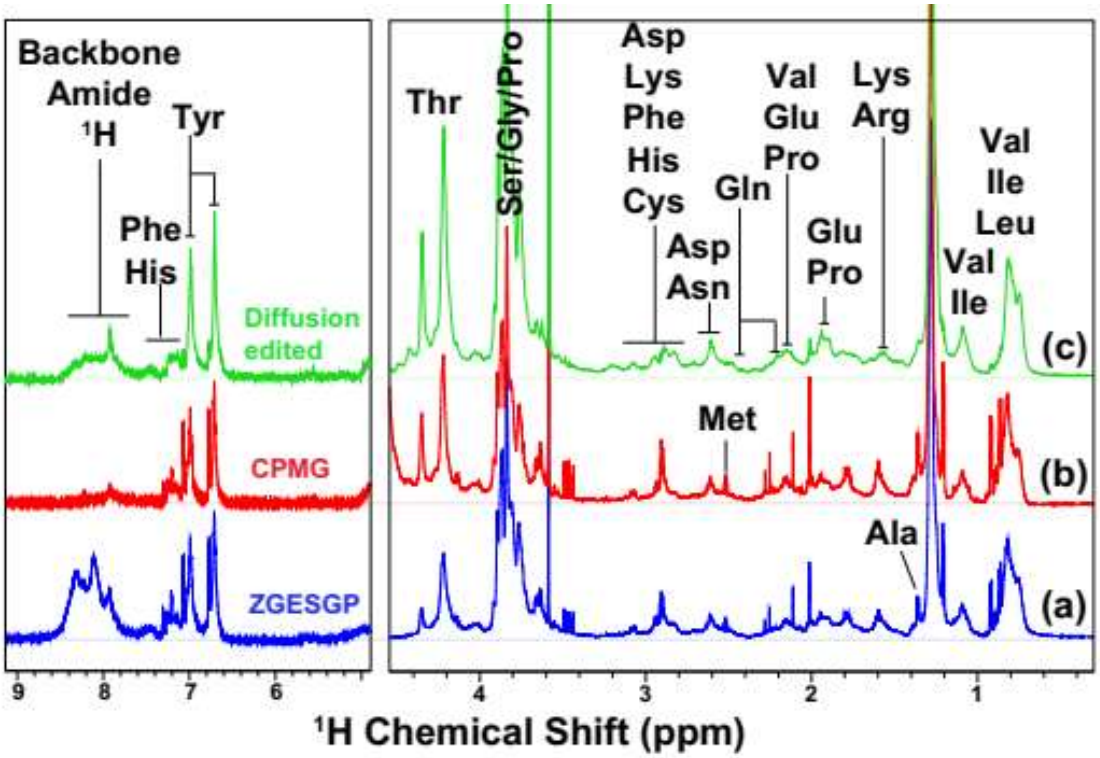

Figure 5: The 1D ¹H NMR spectra of silk SF protein solution recorded on 800 MHz NMR spectrometer. The spectra shown in (a, b and c) represent the ZGESGP, CPMG (T2 relaxation edited) and diffusion edited (filtering of fast diffusing molecules).

Antibacterial study

The antibacterial study confirmed that SF hydrogel has moderate inhibitory activity against *Streptococcus mutans* (gram-positive) and *Salmonella typhi* (gram-negative). The inhibition activity of SF hydrogel against *Streptococcus mutans* was approximately 11, 12, and 15mm at 200, 300, and 400 µg/ml concentrations but did not show any activity at low concentrations (100 µg/ml). Similarly, the inhibition activity of SF hydrogel against *Salmonella typhi* was approximately 12, 13, and 15 mm at 200, 300, and 400 µg/ml concentration (300), but did not show any activity at low concentrations (100 µg/ml). On the other hand, SF hydrogel showed nil activity against *B.cereus* and *P.aeruginosa* at each concentration (100, 200, 300, and 400 µg/ml) as shown in the figure 6 and table 4.

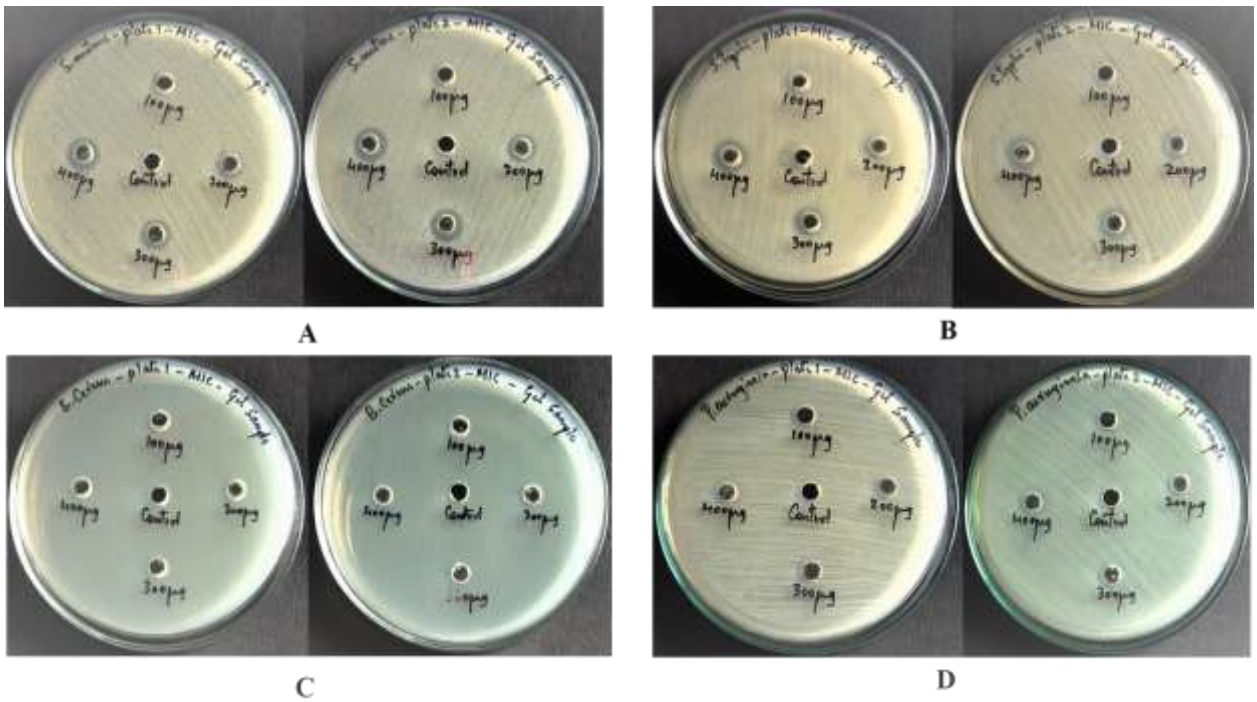

Figure 6: Antibacterial activity of SF hydrogel against (A) *Streptococcus mutans* (B) *Salmonella typhi* (C) *Bacillus cereus and* (D) *Pseudomonas aeruginosa.*

Table 4: MIC of Gel against Organisms

Organisms	Zone of inhibition (in mm) of Gel in µg against *Organisms*							
	100 µg		200 µg		300 µg		400 µg	
Plates	1	2	1	2	1	2	1	2
B.cereus	-	-	-	-	-	-	-	-
S.mutans	-	-	11	11	12	12	14	15
S.typhi	-	-	11	12	13	13	15	14
P.aeruginosa	-	-	-	-	-	-	-	-

Antifungal study

SF hydrogel did not show any activity against *A.flavus* and *A.brassicae* as shown in figure7 and table 5.

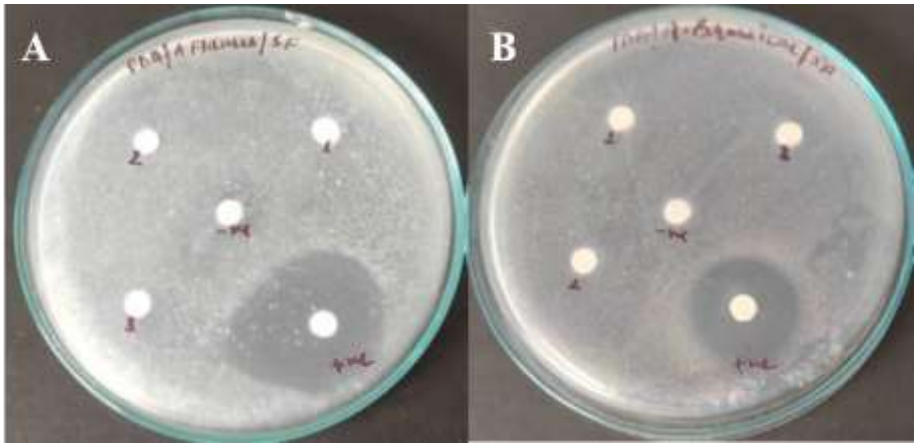

Figure 7: Antifungal activity of SF hydrogel against (A) *A.flavus* and (B) *A. brassicae*

Table 5: Antifungal activity of SF hydrogel against fungal strains

S.No	Sample	Organism	Concentration (µg/ml)	Zone of Inhibition (mm)
1	SF Hydrogel	*A.flavus*	100	nil
			200	Nil
			300	Nil
			Positive control	27
			Negative control	Nil
		A. brassicae	100	Nil
			200	Nil
			300	Nil
			Positive control	27
			Negative control	Nil

Anticancer activity

To determine the effect of silk fibroin hydrogel on the proliferation of human lung cancer cell line A-549 and the optimal dosages, the cells were given a treatment with SF hydrogel at concentrations of 10, 20, 40, and 80 µg/ml for 48 h. The results revealed that SF hydrogel exhibited moderate inhibitory activity on the proliferation of A549 cells at a high concentration of 80 µg/ml (Fig. 9). The images of the cells in normal control, positive control (Adriamycin), and treatment groups (SF hydrogel) were shown in Figure 8 and table 6.

Table 6: The activity of SF hydrogels against the human lung cancer cell line A-549

	A-549 Human Lung Cancer Cell Line															
	Control Growth %															
	Drug Concentrations (µg/ml)															
	Experiment 1				Experiment 2				Experiment 3				Average Values			
	10	20	40	80	10	20	40	80	10	20	40	80	10	20	40	80
SF	71.9	45.1	28.8	15.0	111.9	87.6	83.5	92.1	108.9	85.0	92.2	94.9	97.6	72.6	68.2	67.3
ADR	-11.6	-21.9	0.8	3.7	-15.9	-19.7	-0.7	-15.0	-9.5	-23.1	-6.3	-21.8	-12.3	-21.6	-2.1	-11.0

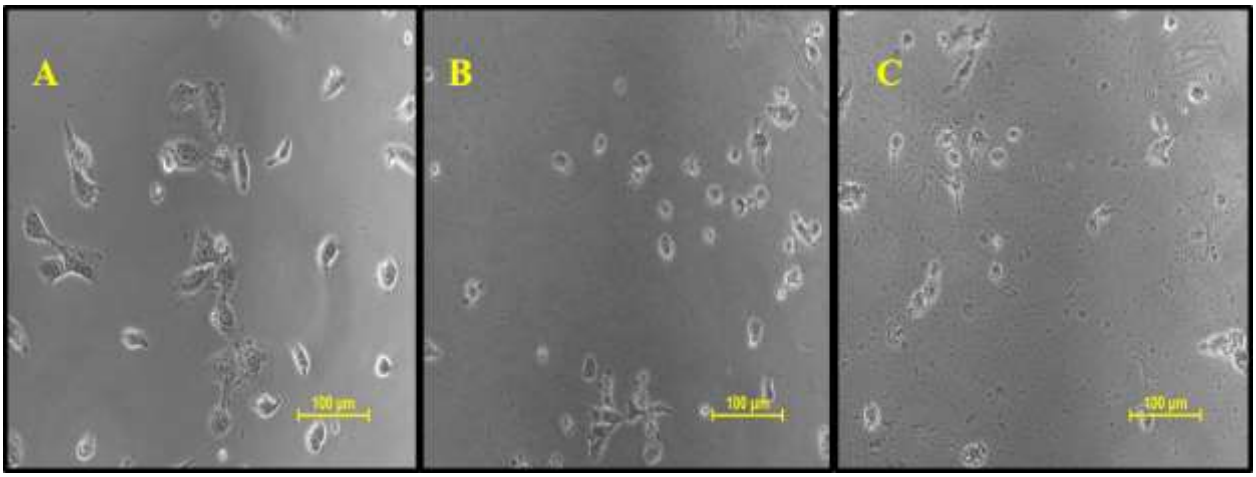

Figure 8: (A) Control group (B). Adriamycin (C). SF hydrogel

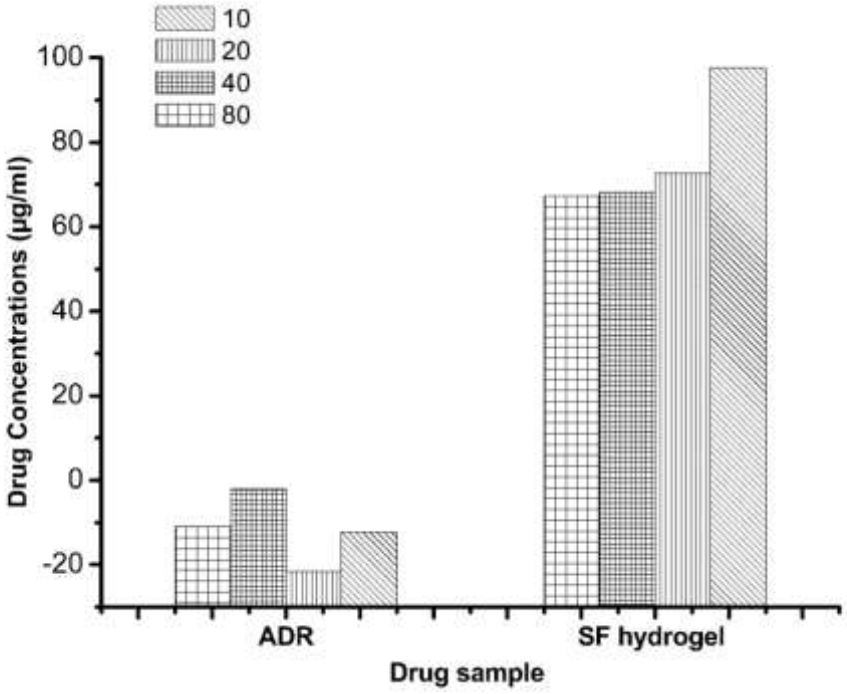

Figure 9: Anticancer activity of SF hydrogel against A549 cancer cell line.

DISCUSSION

SF hydrogel was studied for its characterization and antibacterial, antifungal, and anticancer properties. The characterization of SF hydrogel was done using microscopic, FTIR, and 1H-NMR analysis. Microscopic analysis by SEM, PCM, and fold scope revealed that SF hydrogel has a branching-like structure that makes a scaffold that could be used for drug encapsulation. Our microscopic analysis results are consistent with previous findings, in which researchers confirmed that SF hydrogel had a highly interconnected interweaved fibrous structure due to the presence of β- sheet structure, which is suitable for transporting nutrients and oxygen and contributed to the hydrogel's high integrity and stability[10,34-35]. Similarly, Huang et al, confirmed that SF hydrogels possessed irregular porous structures which increase surface area of network and enables the movement of small molecules into hydrogel [29]. Further FTIR analysis

confirmed the protein nature of SF hydrogel due to the presence amide I, II, and III bonds and also established the beta-sheet at 1230, 1620, and 1514, cm-1 peaks, which are due to gelation. Similarly Zuluaga-Vélez et al**,** also proved the same behavior of **s**ilk fibroin hydrogels and confirmed the amorphous nature of SF hydrogel due to intramolecular antiparallel β-sheet [10]**.** 1D 1H NMR, the major peaks were mainly contributed by the primary structure of the silk fibroin (i.e. alanine, glycine, serine, tyrosine, and valine). As expected, the transformation from α-helix to β-strand enhanced with growing older, eventually forming a β-sheet structure at the occurrence of gelation[33]. Antibacterial studies confirmed that SF hydrogel has moderate inhibition activity against *Streptococcus mutans* (gram-positive) and *Salmonella typhi* (gram-negative). Our antibacterial result is contradictory with some previous results where silk fibroin did not show any activity against S*. aureus S. epidermidis P. aeruginosa* [36,37]. Further, SF hydrogel did not show any activity against A. flavus and *A. brassicae*. Our study shows a similar result to the previous one, where researchers showed that SF film has no antifungal activity [38]**.** The anticancer results revealed that SF hydrogel exhibited moderate inhibitory activity on the proliferation of A549 cells at high concentrations which indicated that SF hydrogel with biocompatible, biodegradable, and regenerative properties could become a wonderful carrier for the anticancer drug without any side effects. In addition, a previous study also confirmed that SF hydrogel has an inhibitory effect on cancer stem cells (CSCs)[39] , antitumor effect, and synergistic tumor therapy effect[40].

CONCLUSION

In this research, we prepared, characterized, and examined the anticancer and antibacterial activity of the SF hydrogel. The chemical shift tendency of 1H-NMR and the spectral line shape reveal that SF hydrogel contains various amino acids, and the presence of beta-sheet structure was confirmed by FTIR analysis. SF hydrogel is porous and having scaffold like structure which is apt for drug loading and drug release. Besides being a well-known the potential drug carrier, the current study showed that SF hydrogel itself is a promising candidate for anticancer and antibacterial activity that can be exploited to the fullest in the future to curb various diseases.

Acknowledgments

We thank Professor Sanjay Singh, the Vice-Chancellor of BBAU, USIC BBAU, and CBMR Lucknow for their support.

Ethics declarations

Since we only conducted an *invitro* studies, no ethical declaration is required for this study.

Conflict of Interest

With regard to the research and publication of this article, the author declares that there are no potential conflicts of interest.

Author Contributions

Vandana Singh**-**experimental design and data analysis and manuscript writing.

Devika Srivastava, Prashant Pandey, Sachin Yadav and Mukesh Kumar–experimental analysis

Dinesh Kumar and Venkatesh Kumar R-manuscript correction and proof reading

Funding Source

This study has no funding support.

REFERENCES

1. Bhardwaj N, Kundu SC. Electrospinning: a fascinating fiber fabrication technique. Biotechnol Adv. 2010; 28(3):325-347. https://doi.org/10.1016/j.biotechadv.2010.01.004

2. Bhardwaj N, Kundu SC. Silk fibroin protein and chitosan polyelectrolyte complex porous scaffolds for tissue engineering applications. Carbohydr Polym. 2011; 85(2):325-333. https://doi.org/10.1016/j.carbpol.2011.02.027

3. Wang Y, Bella E, Lee CS, et al. The synergistic effects of 3-D porous silk fibroin matrix scaffold properties and hydrodynamic environment in cartilage tissue regeneration. Biomaterials. 2010; 31(17):4672-4681. https://doi.org/10.1016/j.biomaterials.2010.02.006

4. Wang H, Yang Z, Adams DJ. Controlling peptidebasedhydrogelation. Mater Today. 2012; 15(11):500-507. https://doi.org/10.1016/S1369-7021(12)70219-5

5. Liao J, Wang B, Huang Y, Qu Y, Peng J, Qian Z. Injectable alginate hydrogel cross-linked by calcium gluconate-loaded porous microspheres for cartilage tissue engineering. ACS Omega. 2017; 2(2):443-454. https://doi.org/10.1021/acsomega.6b00495

6. Yoon JJ, Chung HJ, Park TG. Photo-crosslinkable and biodegradable pluronic/heparin hydrogels for local and sustained delivery of angiogenic growth factor, The Japanese Society for Biomaterials, and The Australian Society for Biomaterials and the Korean Society for Biomaterials. J Biomed Mater Res A. 2007; 83(3):597-605. https://doi.org/10.1002/jbm.a.31271

7. Sun W, Zhang Y, Gregory DA, et al. Patterning the neuronal cells via inkjet printing of self-assembled peptides on silk scaffolds. Prog Nat Sci Mater Int. 2020; 30(5):686-696. https://doi.org/10.1016/j.pnsc.2020.09.007

8. Sun W, Gregory AD. Mhd-Anas-Tomeh AM, ZhaoX. Silk fibroin as a functional biomaterial for tissue engineering. Int J Mol Sci. 2021; 1499:22. https://doi.org/10.3390/ijms22031499

9. Kundu B, Rajkhowa R, Kundu SC, Wang X. Silk fibroin biomaterials for tissue regenerations. Adv Drug Deliv Rev. 2013; 65(4):457-470. https://doi.org/10.1016/j.addr.2012.09.043

10. Zuluaga-Vélez A, Cómbita-Merchán DF, Buitrago-Sierra R, Santa JF, Aguilar-Fernández E, Sepúlveda-Arias JC. Silk fibroin hydrogels from the Colombian silkworm Bombyx mori L: evaluation of physicochemical properties. PLOS ONE. 2019; 14(3):e0213303. https://doi.org/10.1371/journal.pone.0213303

11. Yang C, Li S, Huang X, et al. Silk fibroin hydrogels could be therapeutic biomaterials for neurological diseases. Oxid Med Cell Longev. 2022; 2022:article ID 2076680. https://doi.org/10.1155/2022/2076680

12. Matsumoto A, Chen J, Collette AL, et al. Mechanisms of silk fibroin solGêÆ gel transitions. J Phys Chem B. 2006; 110(43):21630-21638. https://doi.org/10.1021/jp056350v

13. Kim UJ, Park J, Li C, Jin HJ, Valluzzi R, Kaplan DL. Structure and properties of silk hydrogels. Biomacromolecules. 2004; 5(3):786-792. https://doi.org/10.1021/bm0345460

14. Rockwood DN, Preda RC, Yücel T, Wang X, Lovett ML, Kaplan DL. Materials fabrication from Bombyx mori silk fibroin. Nat Protoc. 2011; 6(10):1612-1631. https://doi.org/10.1038/nprot.2011.379

15. Wu W, Wang DS. A fast pH-responsive IPN hydrogel: synthesis and controlled drug delivery. React Funct Polym. 2010;70(9):684-691. https://doi.org/10.1016/j.reactfunctpolym.2010.06.002

16. Wang W, Liu Y, Wang S, et al. Physically cross-linked silk fibroin-based tough hydrogel electrolyte with exceptional water retention and freezing tolerance. ACS Appl Mater Interfaces. 2020; 12(22):25353-25362. https://doi.org/10.1021/acsami.0c07558

17. Jiang S, Yu Z, Zhang L, et al. Effects of different aperture-sized typeI collagen/silk fibroin scaffolds on theproliferation and differentiation of humandental pulp cells. Regen Biomater. 2021; 8(4):rbab028. https://doi.org/10.1093/rb/rbab028

18. Gil ES, Frankowski DJ, Spontak RJ, Hudson SM. Swelling behavior and morphological evolution of mixed gelatin/silk fibroin

hydrogels. Biomacromolecules. 2005a; 6(6):3079-3087. https://doi.org/10.1021/bm050396c

19. Gil ES, Spontak RJ, Hudson SM. Effect of b-sheet crystals on the thermal and rheological behavior of protein-based hydrogels derived from gelatin and silk fibroin. Macromol Biosci. 2005b; 5(8):702-709. https://doi.org/10.1002/mabi.200500076

20. Dou H, Zuo B. Effect of sodium carbonate concentrations on the degumming and regeneration process of silk fibroin. J Text Inst. 2015; 106(3):311-319.olymers. doi:10.1080/00405000.2014.919065.

https://doi.org/10.1080/00405000.2014.919065

21. Hasturk O, Jordan KE, Choi J, Kaplan DL. Enzymatically crosslinked silk and silk-gelatin hydrogels with tunable gelation kinetics, mechanical properties and bioactivity for cell culture and encapsulation. Biomaterials. 2020; 232:119720. https://doi.org/10.1016/j.biomaterials.2019.119720

22. Ghalei S, Handa H. A review on antibacterial silk fibroin-based biomaterials: current state and prospects. Mater Today Chem. 2022; 23:100673, ISSN 2468-5194. https://doi.org/10.1016/j.mtchem.2021.100673

23. Ribeiro VP, Silva-Correia J, Gonçalves C, et al. Rapidly responsive silk fibroin hydrogels as an artificial matrix for the programmed tumor cells death. PLOS ONE. 2018; 13(4):e0194441. https://doi.org/10.1371/journal.pone.0194441

24. Belay B, Koivisto JT, Parraga J, et al. Optical projection tomography as a quantitative tool for analysis of cell morphology and density in 3D hydrogels. Sci Rep. 2021; 11(1):6538. https://doi.org/10.1038/s41598-021-85996-8

25. Pandey P, Mishra A, Pandey J. Effect on immunity and overall tissue health of stinging catfish, Heteropnuestes fossilis (Bloch, 1974) in curcumin medium. Indian J Nutr Diet. 2022; 29282. 59(2):169-186. https://doi.org/10.21048/IJND.2022.59.2.29282

26. Nongpiur CG, Tripathi DK, Poluri KM, Rawat H, Kollipara MR. Ruthenium, rhodium and iridium complexes containing diazafluorene derivative ligands: synthesis and biological studies. J Chem Sci. 2022; 134(1):1-4. https://doi.org/10.1007/s12039-021-02004-2

27. Singh V, Pranjali P, Raj R, et al. Improved antimicrobial activity of zinc-oxide Nanoparticles in peritoneal dialysis fluid using Silk Fibroin Protein coating. Mater Res Innov. 2022:1-8. https://doi.org/10.1080/14328917.2022.2157984

28. Kode J, Kovvuri J, Nagaraju B, et al. Synthesis, biological evaluation and molecular docking analysis of phenstatin based indole linked chalcones as anticancer agents and tubulin polymerization inhibitors. Bioorg Chem. 2020; 105:104447. https://doi.org/10.1016/j.bioorg.2020.104447

29. Huang Y, Zhang B, Xu G, Hao W. Swelling behaviours and mechanical properties of silk fibroin-polyurethane composite hydrogels. Compos Sci Technol. 2013; 84:15-22. https://doi.org/10.1016/j.compscitech.2013.05.007

30. Zhang H, Li Ll, Dai FY, Fy. et al. Preparation and characterization of silk fibroin as a biomaterial with potential for drug delivery. J Transl Med. 2017; 10:117. https://doi.org/10.1186/1479-5876-10-117

31. Yao J, Ohgo K, Sugino R, Kishore R, Asakura T. Structural Analysis of Bombyx mori Silk Fibroin Peptides with formic acid Treatment Using High-Resolution Solid-State 13C NMR Spectroscopy. Biomacromolecules. 2004;5(5):1763-1769. https://doi.org/10.1021/bm049831d

32. Asakura T, Suzuki Y, Nakazawa Y, Yazawa K, Holland GP, Yarger JL. Silk structure studied with nuclear magnetic resonance. Prog Nucl Magn Reson Spectrosc. 2013; 69:23-68. https://doi.org/10.1016/j.pnmrs.2012.08.001

33. Le Zainuddin TT, Park Yoosup, Chirila TV, Halley PJ, Whittaker AK. The behavior of aged regenerated Bombyx mori silk fibroin solutions studied by 1H NMR and rheology, Biomaterials. 2008; 29(32):4268-4274, ISSN 0142-9612. https://doi.org/10.1016/j.biomaterials.2008.07.041

34. Singh YP, Bhardwaj N, Mandal BimanB. Potential of agarose/silk fibroin blended hydrogel for in vitro cartilage tissue engineering. ACS Appl Mater Interfaces. 2016; 8(33):21236-21249. https://doi.org/10.1021/acsami.6b08285

35. Wu X, Hou J, Li M, Wang J, Kaplan DL, Lu S. Sodium dodecyl sulfate-induced rapid gelation of silk fibroin. Acta Biomater. 2012; 8(6):2185-2192. https://doi.org/10.1016/j.actbio.2012.03.007

36. Calamak S, Aksoy EA, Ertas N, Erdogdu C, Sagıroglu M, Ulubayram K. Ag/silk fibroin nanofibers: effect of fibroin morphology on Ag+ release and antibacterial activity. Eur Polym J. 2015; 67:99-112. https://doi.org/10.1016/j.eurpolymj.2015.03.068

37. Wang X, Ding Z, Wang C, et al. Bioactive silk hydrogels with tunable mechanical properties. J Mater Chem B. 2018; 6(18):2739-2746. https://doi.org/10.1039/C8TB00607E

38. Yerra A, Mamatha DM. Antibiotic-based silk fibroin films for burn wound healing. Polym Adv Technol. October 24 2020. https://doi.org/10.1002/pat.5137

39. Wu P, Liu Q, Wang Q, et al. Novel silk fibroin nanoparticles incorporated silk fibroin hydrogel for inhibition of cancer stem cells and tumor growth. Int J Nanomedicine. 2018:17; 13:5405-5418, PubMed: 30271137, PubMed Central: PMC6149978. https://doi.org/10.2147/IJN.S166104

40. Gou Shuangquan, Xie Dengchao, Ma Y, et al. Injectable, thixotropic, and multiresponsive silk fibroin hydrogel for localized and synergistic tumor therapy. ACS Biomater Sci Eng. 2020; 6(2):1052-1063. https://doi.org/10.1021/acsbiomaterials.9b01676